

Chemical Looping Steam Methane Reforming Process Using NiFe_2O_4 as Oxygen Carrier for Hydrogen Production

Zhongrui Gai^{1,2}, Yang Li^{2,3}, Qiong Rao^{2,3}, Yuanhui Shen^{2,3}, Yunlian Liu^{2,3}, Ying Pan^{2*}

1 State Key Laboratory of Multiphase Flow in Power Engineering, Xi'an Jiaotong University, Xi'an 710049, Shaanxi, China

2 Institute of Engineering Thermophysics, Chinese Academy of Sciences, Beijing 100190, PR China

3 University of Chinese Academy of Sciences, Beijing 100049, China

(*Corresponding Author: panying@iet.cn)

ABSTRACT

Chemical looping steam methane reforming (CLSMR) using metal oxide as oxygen carrier is regarded as an promising approach for hydrogen production, offering reduced costs and lower CO_2 emissions compared to conventional steam methane reforming process. In this study, we proposed a multi-step chemical looping steam methane reforming process using NiFe_2O_4 as oxygen carrier (OC) for hydrogen production. Simulation model of the proposed cycle was developed using Aspen Plus. Experiments on fixed-bed reactor have been conducted to validate the reliability of simulation model. The effect of key process parameters has been evaluated. We found that the presented CLSMR process realized over 85% CH_4 conversion in reduction step at 700 °C and more than 1.6 times of total product generation rate than that of $\text{FeO}/\text{Fe}_3\text{O}_4$ system at 900 °C in experiments. In terms of simulation model, 86.5% of methane to fuel efficiency and 66.9% of net efficiency could be obtained. The results demonstrate the proposed process has the potential to make advances in energy-efficient hydrogen production.

Keywords: Hydrogen production, Chemical looping steam methane reforming (CLSMR), NiFe_2O_4 , Process simulation

OC	Oxygen Carrier
FR	Fuel Reactor
SR	Steam Reactor
AR	Air Reactor
WGS	Water Gas Shift
PSA	Pressure Swing Adsorption
MS	Mass Spectrometer
GC	Gas Chromatograph
HTS	High Temperature Shift
LTS	Low Temperature Shift

Symbols

T	Temperature
\dot{n}	Molar amount
x	Gas fraction
i	Gas type
V	Volume of dry gas product
b	Baseline
m	Mass
t	Reaction time
in	Input
out	Output
H	Input heat
R	Heat recovery
S	Steam
W	Work
η_e	Power generation efficiency

NONMENCLATURE

Abbreviations

SMR	Steam Methane Reforming
CLSMR	Chemical Looping Steam Methane Reforming
SE	Sorption Enhanced

1. INTRODUCTION

Due to the greenhouse gas effect caused by fossil fuel combustion, renewable energy is increasingly favored for substitution of fossil fuel. Hydrogen is considered an alternative and environmentally friendly renewable fuel, it can serve as a feedstock in ammonia

synthesis, methanol production and the generation of electricity via fuel cells [1].

Typically, H₂ is produced using the steam methane reforming (SMR), which is the most widely used technology for the industrial production of hydrogen and accounts for more than half of the world hydrogen production. However, the SMR process is a highly endothermic catalytic reaction, high energy demand in the reforming reactor is needed and the catalyst used in the process could be deactivated due to coking. Moreover, substantial quantities of CO₂ are produced as a byproduct in this procedure [2].

Chemical looping steam methane reforming (CLSMR) has emerged as an attractive process for hydrogen production [3]. As it enables achievement of both syngas and high purity hydrogen via the recycling of oxygen carrier (OC, typically, transition metal oxide) in the redox process. This process mitigates irreversible separation losses and enhances energy utilization efficiency compared with conventional steam reforming.

Research of chemical looping steam methane reforming has been widely conducted. Ortiz et al. [4] performed a thermodynamics analysis and process simulation of CLSMR process using FeO/Fe₃O₄ redox pair as OC to find optimal operating conditions for high H₂ and syngas production. Saithong et al. [5] present an integrated sorption-enhanced chemical looping steam methane reforming (SE-CLSMR) process with Fe-based OC for H₂ production, the effect of key parameters is studied in detail. He et al. [3] proposed a hybrid solar-redox system of CLSMR for cogeneration of liquid fuels and hydrogen, 95% conversion of methane is achieved in the iron oxide reduction step at 900 °C.

OCs used in previous studies of CLSMR process are generally single metal oxide, especially Fe-based OCs. Fe-based OCs have been widely used due to their notable attributes such as strong resistance to attrition, minimal sintering risk, and high heat carrier capacity. Nonetheless, its low reaction kinetics have been observed, leading to low fuel conversion efficiency [6].

In comparison to single metal oxides, the composite metal oxides generally showcase exceptional oxygen transfer capacity, good thermal stability and extensive specific surface area because of the synergistic effects between the polymetallic elements. NiFe₂O₄ is a representative Fe-Ni bimetallic oxide with a cubic inverse-spinel structure, attributed to its unique crystal structure, it exhibits excellent catalytic and redox properties [7]. NiFe₂O₄ can not only address the high expense and toxicity associated with Ni-based OCs but also improve the reactivity of Fe-based OCs. Considering

the overall performance, NiFe₂O₄ could be a suitable candidate for CLSMR process.

In current study, we proposed a multi-step chemical looping steam methane reforming process using NiFe₂O₄ as oxygen carrier for high-purity hydrogen production. In experimental studies, high methane conversion was achieved in the OC reduction step at lower temperature in contrast with typical FeO/Fe₃O₄ cycles. Results from experimental studies were observed in good accordance with the outcomes of simulation calculation. In terms of simulation model, higher methane to fuel efficiency and net efficiency could be obtained compared with conventional SMR process. The effect of key parameters such as the fuel reactor temperature (T_{FR}), molar feeding ratio of steam to methane (n_{SFR}/n_{CH_4}) and oxygen carrier to methane (n_{oc}/n_{CH_4}) has been evaluated were investigated.

2. EXPERIMENTAL AND SIMULATION METHODS

2.1 Process description

The proposed CLSMR process primarily includes three steps [8]: OC reduction step, steam oxidation step and air oxidation step.

In the first step, spinel nickel ferrite material NiFe₂O₄ is used to convert methane into syngas in a fuel reactor (FR), which reduces NiFe₂O₄ to Ni and Fe/FeO (or FeO_{1-δ}). In the second step, reduced ferrite material from the previous step is re-oxidized to Fe₃O₄ by steam in a steam reactor (SR), producing H₂ and eliminate carbon deposits. In the final step, the mixture phase of Ni and Fe₃O₄ is oxidized back to the original spinel phase of NiFe₂O₄ by air in the air reactor (AR).

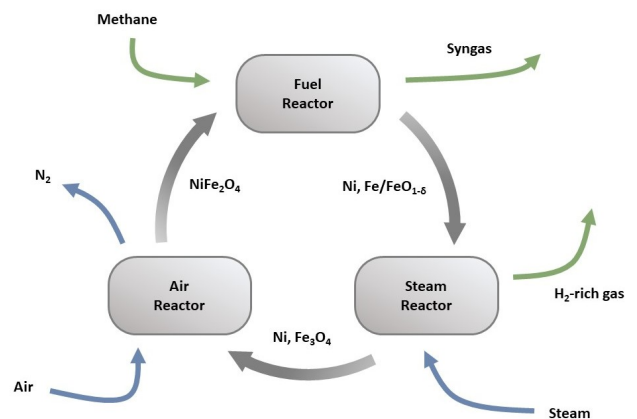


Fig. 1 Simplified schematic of the multi-step CLSMR process.

2.2 Experimental procedure

2.2.1 Materials and preparation

Nickel ferrite (NiFe_2O_4) with 40wt% Al_2O_3 support is used as OC of CLSMR process. The NiFe_2O_4 powder sample was synthesized by sol-gel method [9]. The metal nitrates $\text{Ni}(\text{NO}_3)_2 \cdot 6\text{H}_2\text{O}$ and $\text{Fe}(\text{NO}_3)_3 \cdot 9\text{H}_2\text{O}$ were employed as the metal sources. Desired amounts of metal nitrates and citric acid were dissolved in deionized water under constant stirring until reaching complete dissolution. Then the mixture was stirred with a magnetic machine at 80 °C to get the gel which was then dried for 3 h at 130 °C in a drying oven and calcined for 4 h at 850 °C in air. Finally, the particles were crushed and sieved to get NiFe_2O_4 powder. The synthesized NiFe_2O_4 powder was uniformly mixed with Al_2O_3 powder at a mass ratio of 3:2 to get the resultant OC.

2.2.2 Experimental set-up

Experiments for CLSMR were carried out in a fix-bed quartz tube reactor. Before the reaction, 0.25 g of OC powder is loaded, the reactor is heated under argon flow of 20 ml min^{-1} . Once the desired temperature is reached, 2 ml min^{-1} of CH_4 is introduced into the reactor for OC reduction. CH_4 injection is stopped after 30 min, and the water-splitting reaction is carried out after the residue gas from OC reduction step has been completely purged with Ar. Then 5 $\mu\text{L min}^{-1}$ H_2O is injection for 15 min and heated to steam by a steam generator. During the OC reduction step and steam oxidation step, 6 ml min^{-1} of argon is used as the internal standard. The reaction is stopped when H_2 concentration is below 2%. Afterwards, 20 ml min^{-1} of air is purged into the reactor to conduct air oxidation.

Compositions of the gas exiting the reactor are determined using both mass spectrometer (MS) and gas chromatograph (GC). The crystal phases of the metal oxides are acquired using X-ray powder diffraction (XRD) with $\text{Cu-K}\alpha$ radiation ($\lambda=0.15418$ nm) in the $2\theta=20\text{-}80^\circ$ angle range. Details about the fix-bed quartz tube reactor have been reported earlier [10].

2.3 Process modelling

Aspen Plus V11 was used for the process modelling. The simulation model developed for the CLSMR process is shown in Fig. 2.

The minimization of Gibbs free energy led to determining the product equilibrium composition at specific operating conditions. Detailed system setup, unit operation models are summarized in Table 1.

The model could be divided into 4 sections: CLSMR section, WGS section, PSA section and HR section.

Similar to the process mentioned above, the CLSMR section includes fuel reactor (FR), steam reactor (SR), air reactor (AR) and separators. The cold stream of feed CH_4 and H_2O was heated and vaporized by hot stream off these reactors to maximize heat recovery and minimize external heat requirement.

The syngas produced from FR and SR is introduced into water-gas shift (WGS) section to increase the hydrogen content, the WGS section includes two WGS reactor [11]: one at high temperature (HTS), and the other at low temperature (LTS). In the HTS reactor, CO has a low conversion with quick kinetics, because it

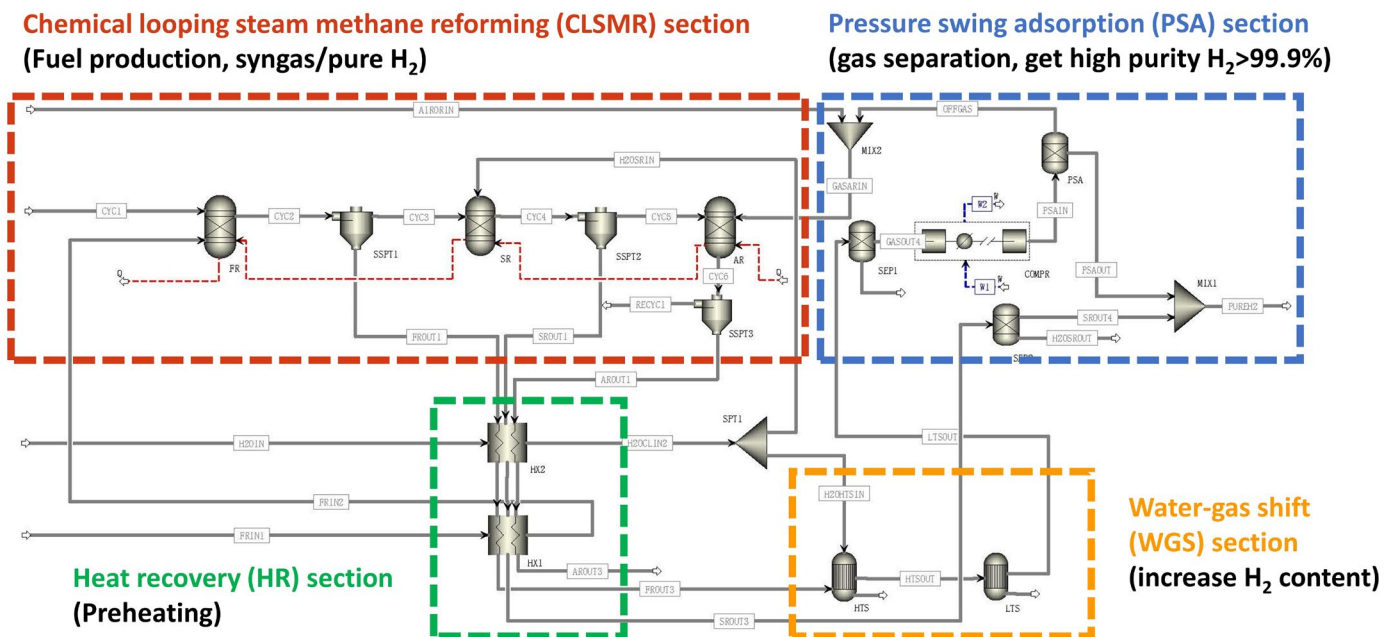


Fig. 2 Flowsheet of the multi-step CLSMR process using NiFe_2O_4 as OC.

remains impossible to go beyond the equilibrium. Then the LTS reactor is utilized to secure higher conversion.

Table 1 Aspen plus model setup.

Overall Setup	
Property method (free water method)	RK-SOAVE (IAPWS-95)
Solid components	C, NiFe ₂ O ₄ , Ni, NiO, Fe, Fe _{0.947} O, Fe ₃ O ₄ , Fe ₂ O ₃
Gas components	CH ₄ , CO, CO ₂ , H ₂ , H ₂ O, N ₂ , O ₂
Solution strategy	Sequential Modular
Unit operations models	
FR/SR/AR	RGibbs
WGS reactor	REquil
PSA	Sep
Pressure changers	MCompr
Heat exchangers	MHeatX
Mixers/Splitters	Mixer/FSplit, SSplit, Sep

The H₂-rich gas acquired from WGS section is compressed and purified using a pressure swing adsorption (PSA) unit into a final product of high-purity H₂ (>99.9%) [12]. A quantity of off-gas from the PSA is delivered to AR for combustion to compensate the heat demand of FR and SR.

Table 2 Key assumptions and simulation parameters.

Parameter	Value	
	Base case condition	Studied ranges
n_{CH_4} input (kmol/h)	1	
n_{SR} input (kmol/h)	1.2	
n_{OC} input (kmol/h)	0.25	0-1
n_{SR} input (kmol/h)	0	0-3
Reactor temperature (°C)	FR: 700 SR: 600 AR: 800 HTS: 350 LTS: 200	FR: 650-900 AR: 800-900
PSA	95% H ₂ recovery [13]	
Compressor	Isentropic efficiency: 80% Outlet pressure: 20 bar	
Heat recovery	Pinch point: >15 °C	

As is listed in Table 2, Key assumptions and simulation parameters of base case condition have a rational setup, which is a proportionally scaled up of the experimental parameters. Studied ranges are used for sensitive analysis, which is conducted to investigate the effect of different operating conditions.

2.4 Calculation Formula

Quantitative parameters for evaluating the redox experiments and simulations are summarized in Table 3.

Table 3 Quantitative parameters.

Parameter	Equations
Production rate	$\frac{\int_0^t x_i V_{total} dt - \int_0^t x_{i,b} V_{total} dt}{m \cdot t}$
CH ₄ conversion	$\left(1 - \frac{\dot{n}_{CH_4,out}}{\dot{n}_{CH_4,in}} \right) \times 100\%$
H ₂ purity	$\left(\frac{\dot{n}_{H_2,out}}{\dot{n}_{H_2,out} + \dot{n}_{CO_2,out} + \dot{n}_{CO,out} + \dot{n}_{CH_4,out}} \right) \times 100\%$
Syngas yield	$\left(\frac{\dot{n}_{H_2,out} + \dot{n}_{CO,out}}{\dot{n}_{CH_4,in}} \right) \times 100\%$
Methane to fuel efficiency	$\left(\frac{\dot{n}_{H_2,out} \cdot LHV_{H_2}}{\dot{n}_{CH_4,out} \cdot LHV_{CH_4}} \right) \times 100\%$
Net energy efficiency	$\left(\frac{\dot{n}_{H_2,out} \cdot LHV_{H_2}}{\dot{n}_{CH_4,out} \cdot LHV_{CH_4} + (Q_H - Q_R) + \frac{W_{PSA}}{\eta_e}} \right) \times 100\%$

3. RESULTS AND DISCUSSION

3.1 Experimental results and model validation

The real-time production rate of dry gas product is showed in Fig. 3. It could be seen that in first 10 min the gas product mainly consisted of CH₄, CO, CO₂, and CH₄, CO₂ gradually declined in the following 20 min. Production rate of H₂ increased rapidly to 5.3 mmol min⁻¹ g⁻¹ from 10th min, and stopped after 30th min. After steam injection at 50th min, H₂ appeared and increased to 1.3 mmol min⁻¹ g⁻¹ without generation of CO, CO₂ and CH₄, which means the carbon deposits in OC reduction step have been fully removed. Air was purged into the reactor after H₂O oxidation, retained gases were then

swept out. Settings and results of above experiments and reference are summarized in Table 4.

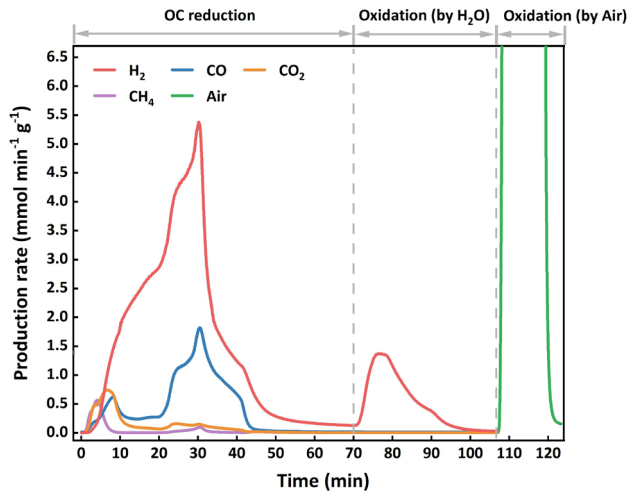


Fig. 3 Measured dry gas production rate during the multi-step CLSMR reaction. (FR/SR/AR Temperature: 750 °C/600 °C/800 °C).

Table 4 Settings and experiment results in this work and reference work.

Operation condition	Exp	Ref
Temperature (°C)	700	900
Pressure (bar)	1	1
n_{OC}/n_{CH_4}	0.26	0.26
n_{SFR}/n_{CH_4}	0	0
CH ₄ conversion (%)	88.5	95.3
Syngas yield (%)	69.7	59
n_{H_2}/n_{CO}	5.6	1.9
Total product generation rate (J g ⁻¹ min ⁻¹)	81.7	62.7

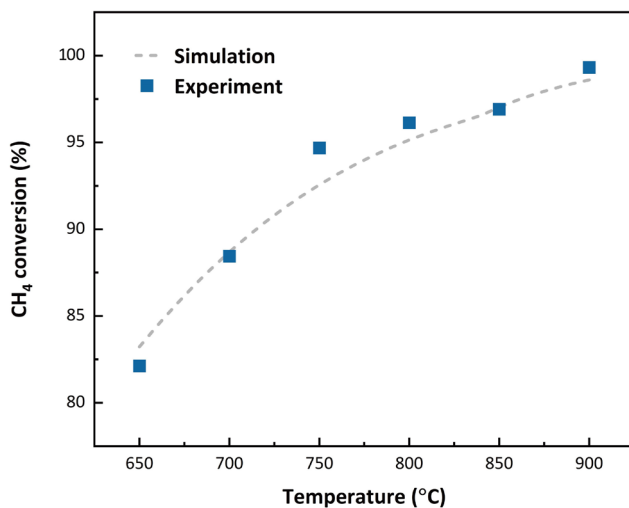


Fig. 4 CH₄ conversion as function of temperature. Dashed line represents the simulated results, while Dots represent the experimental results.

In order to utilize the model for calculations and predictions effectively to acquire optimal operating conditions, it is essential to perform a reliable validation of the model, while CH₄ conversion is considered as the valid proofs in this work. Fig. 4 shows the resulting CH₄ conversions from the experimental results and simulation data of the CLSMR process. It could be found that the model predictions were in good agreement with the experimentally obtained CH₄ conversions. This indicates that the thermodynamic model was basically credible and could be employed to predict gas composition.

Another crucial point that needs validation is the spinel phase of OC after cycles [13,14]. As is depicted in Fig. 5, the crystal phase of fresh OC sample and OC sample after 10 cycles were examined by X-ray diffraction (XRD). The fresh sample is mainly composed of spinel NiFe₂O₄ phase and Al₂O₃ phase, which confirms the purity of OC. It could be found that the spinel NiFe₂O₄ structure is well maintained, little phase of other species is observed after 10 cycles. It indicates that the multi-step CLSMR process could be achieved, and the addition of Al₂O₃ support could significantly improve the stability of NiFe₂O₄ in CLSMR cycles.

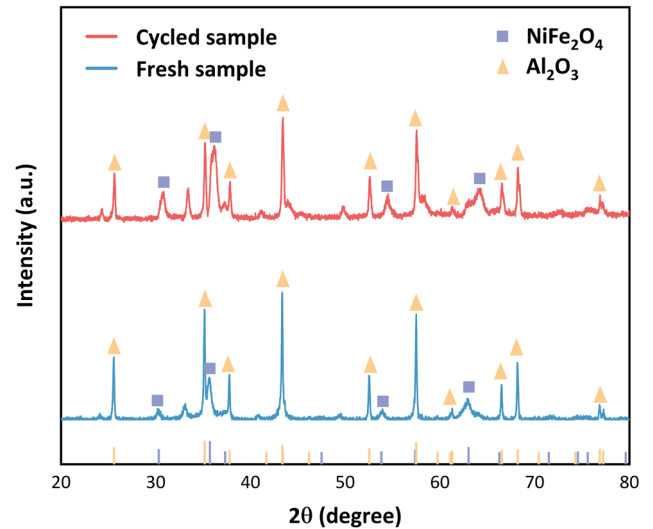


Fig. 5 The XRD pattern of fresh sample and sample after 10 cycles.

3.2 Process simulation

As is listed in Table 5, simplified heat calculations were performed. Among the energy input, work used for PSA accounts for nearly 20% of energy input, leading to decrease in net efficiency of overall system. Energy for heating could be effectively compensated by heat generated from OC oxidation and off-gas combustion in the air reactor, the net efficiency benefits from that while the methane to fuel efficiency decreases.

Table 5 Energy analysis of proposed system in base case condition.

Items	Value	Ratio
Input		
Methane (kW)	222.2	77.4%
Energy for heating (kW)	10.6	3.7%
Energy for Work (kW)	54.3	18.9%
Output		
Hydrogen (kW)	192.2	100%
Efficiency		
Methane to fuel efficiency (%)		86.5%
Net efficiency (%)		66.9%

In general, the methane to fuel efficiency is significantly higher than that of conventional methane reforming process, which are typically 70% [3]. The net efficiency is slightly higher than that of typical FeO/Fe₃O₄ redox pair system.

3.2.1 Effects of T_{FR}

Fig. 6 (a)-(b) shows the effect of T_{FR} in the range of 600-900 °C on the gas yield in the FR and SR, CH₄ conversion, net efficiency and H₂ purity.

The results show that with the increase of T_{FR} , the production amount of H₂ and CO in FR increases. This could be explained by the significant increment of CH₄ conversion, and the H₂ purity of SR benefits a lot from the increase of T_{FR} because of the diminished carbon deposits. The net efficiency appears to be flat after T_{FR} reached 700 °C, it denotes that the gains in increasement of hydrogen yield were offset by increased work and heat demand.

3.2.2 Effect of n_{oc}/n_{CH_4}

Fig. 7 (a)-(b) shows the effect of n_{oc}/n_{CH_4} in the range of 0-1 on the gas yield in the FR and SR, CH₄ conversion, net efficiency and H₂ purity.

The results show that with the increase of input OC amount, the production amount of CO and CO₂ in FR increased. It indicates that complete oxidation of CH₄ becomes dominant, while the proportion of the partial oxidation decreases. H₂ production in SR appears to increase at first but decrease from $n_{oc}/n_{CH_4}=0.7$. This could be explained that the reduced OC is increased initially but excess at last, which leads to the decrease of OC in SR. It could be derived that CH₄ conversion increase with n_{oc}/n_{CH_4} , but excess OC causes a reduction in hydrogen production. Hence, an optimal point for net efficiency could be found at $n_{oc}/n_{CH_4}=0.25$.

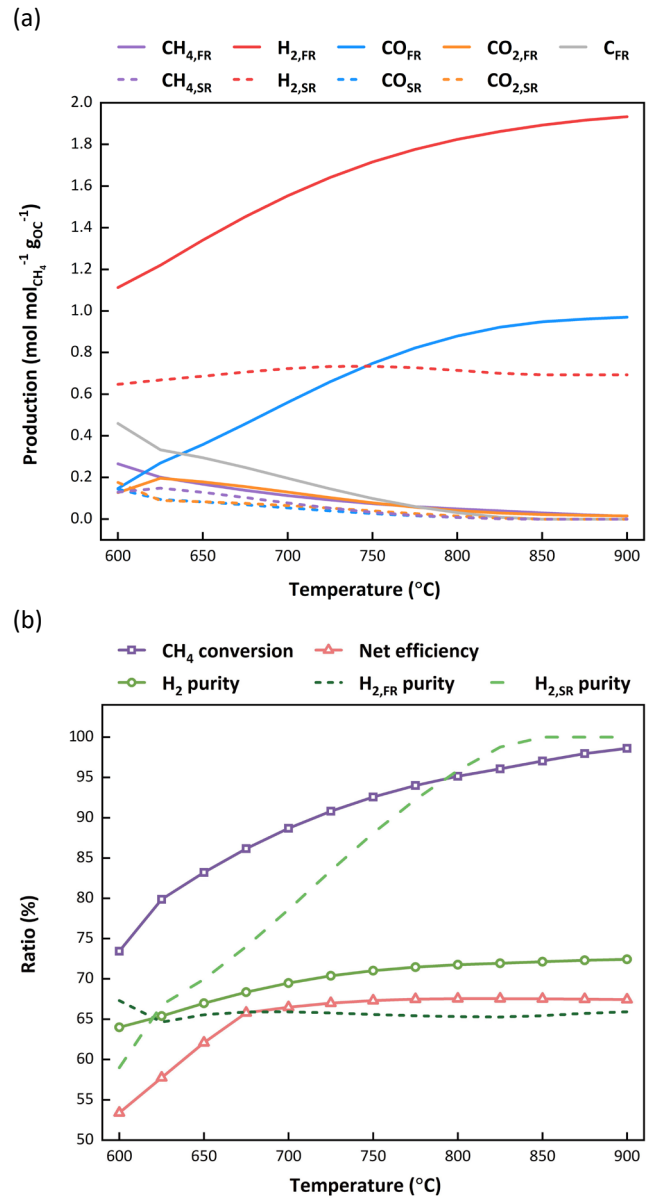


Fig. 6 The effect of T_{FR} on (a) Outlet gas composition of FR and SR. (b) CH₄ conversion, net efficiency, H₂ purity of mixed gas, outlet gas of FR and SR at $n_{oc}/n_{CH_4}=0.26$, $n_{SFR}/n_{CH_4}=0$.

3.2.3 Effect of n_{SFR}/n_{CH_4}

Fig. 8 (a)-(b) shows the effect of n_{SFR}/n_{CH_4} in the range of 0-3 on the gas yield in the FR and SR, CH₄ conversion, net efficiency and H₂ purity.

The results show that with the increase of H₂O injection amount, the production amount of H₂ in FR increased significantly. CO₂ production amount increases because of the shifting of WGS reaction driven by the addition of H₂O. An appropriate amount of steam can effectively eliminate carbon deposition and give rise to H₂ purity both in FR and SR. It is worth noting that the H₂

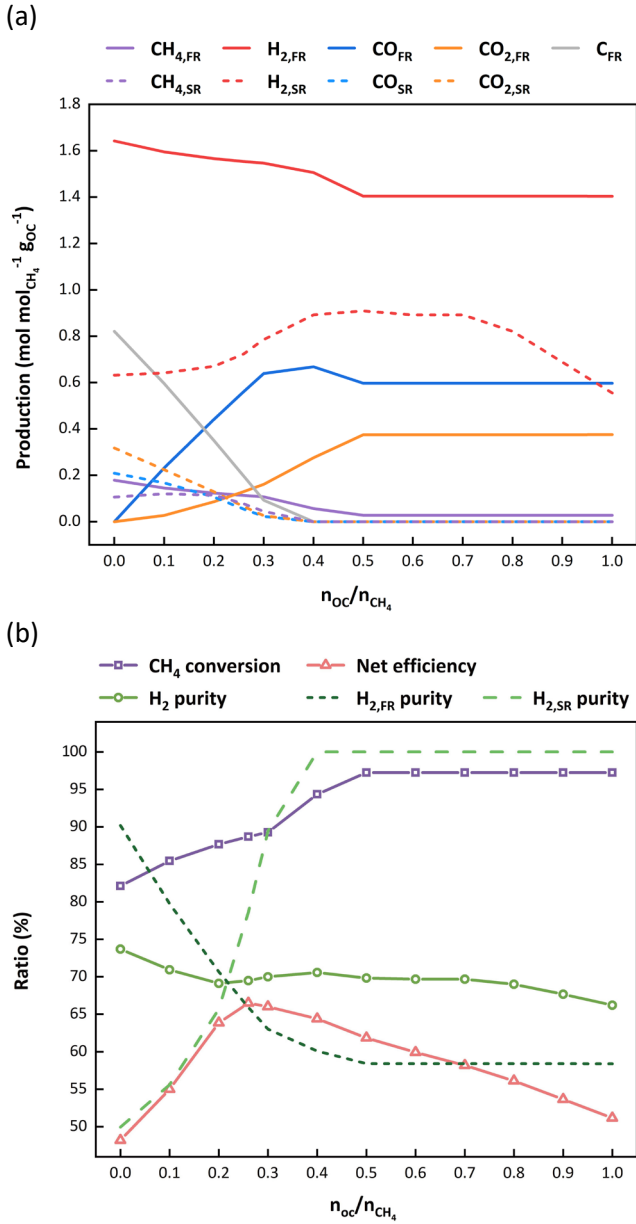


Fig. 7 The effect of n_{OC}/n_{CH_4} on (a) Outlet gas composition of FR and SR. (b) CH₄ conversion, net efficiency, H₂ purity of mixed gas, outlet gas of FR and SR at $T_{FR}=700$ °C, $n_{SFR}/n_{CH_4}=0$.

production in SR decrease when $n_{SFR}/n_{CH_4} > 1$, it could be explained that when n_{SFR}/n_{CH_4} is excess, FeO from reduction step would be re-oxidized to Fe₃O₄ in an enriched H₂O environment, thus the H₂ yield of SR decreases.

The net efficiency appears to be flat, it could be found that the gains in increasement of hydrogen yield were offset by increased heat demand to generate steam.

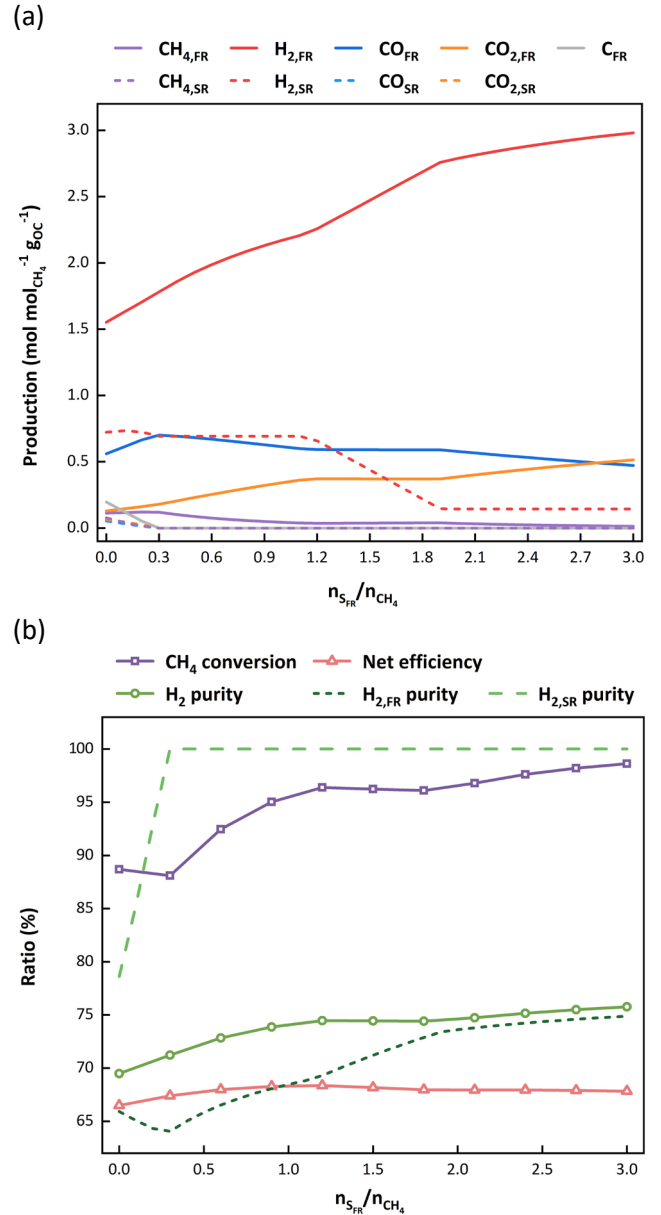


Fig. 8 The effect of n_{SFR}/n_{CH_4} on (a) Outlet gas composition of FR and SR. (b) CH₄ conversion, net efficiency, H₂ purity of mixed gas, outlet gas of FR and SR at $T_{FR}=700$ °C, $n_{OC}/n_{CH_4}=0.26$.

4. CONCLUSIONS

The multi-step CLSMR process using NiFe₂O₄ as OC was investigated using both experiments and thermodynamic approach. The simulation model was effectively validated by data acquired from experiments on fix-bed reactor. XRD results showed the stability of OC after cycles. It was found that the presented CLSMR cycle realized over 85% CH₄ conversion in reduction step at 700 °C and more than 1.6 times of total product generation rate than that of FeO/Fe₃O₄ system at 900 °C. In base case condition, 86.5% of methane to fuel efficiency and 66.9% of net efficiency were achieved.

Sensitivity analysis of key process parameters T_{FR} , n_{oc}/n_{CH_4} , n_{SFR}/n_{CH_4} was performed, optimal condition of $n_{oc}/n_{CH_4}=0.25$, $T_{FR}>700$ °C, $n_{SFR}/n_{CH_4}<1$ was obtained. The results showcase the proposed CLSMR process as a potent approach for efficient hydrogen production.

ACKNOWLEDGEMENT

The authors would like to acknowledge the support by National Natural Science Foundation of China (NSFC) (Grant No. 51888103, No. 52176026, and No. 52241601).

DECLARATION OF INTEREST STATEMENT

The authors declare that they have no known competing financial interests or personal relationships that could have appeared to influence the work reported in this paper. All authors read and approved the final manuscript.

REFERENCE

- [1] FEATURE The future of fuel: The future of hydrogen. 2012.
- [2] Habibi R, Mehrpooya M. A novel integrated Ca-Cu cycle with coal/biomass gasification unit for clean hydrogen production. *Energy Convers Manag* 2021;228. <https://doi.org/10.1016/j.enconman.2020.113682>.
- [3] He F, Trainham J, Parsons G, Newman JS, Li F. A hybrid solar-redox scheme for liquid fuel and hydrogen coproduction. *Energy Environ Sci* 2014;7:2033–42. <https://doi.org/10.1039/c4ee00038b>.
- [4] López-Ortiz A, Meléndez-Zaragoza MJ, Collins-Martínez V. Hydrogen production by a Fe-based oxygen carrier and methane-steam redox process: Thermodynamic analysis. *Int J Hydrogen Energy* 2017;42:30195–207. <https://doi.org/10.1016/j.ijhydene.2017.07.130>.
- [5] Saithong N, Authayanun S, Patcharavorachot Y, Arpornwichanop A. Thermodynamic analysis of the novel chemical looping process for two-grade hydrogen production with CO₂ capture. *Energy Convers Manag* 2019;180:325–37. <https://doi.org/10.1016/j.enconman.2018.11.003>.
- [6] Huang Z, Deng Z, He F, Chen D, Wei G, Zhao K, et al. Reactivity investigation on chemical looping gasification of biomass char using nickel ferrite oxygen carrier. *Int J Hydrogen Energy* 2017;42:14458–70. <https://doi.org/10.1016/j.ijhydene.2017.04.246>.
- [7] Huang Z, Deng Z, Chen D, Wei G, He F, Zhao K, et al. Exploration of Reaction Mechanisms on Hydrogen Production through Chemical Looping Steam Reforming Using NiFe₂O₄ Oxygen Carrier. *ACS Sustain Chem Eng* 2019;7:11621–32. <https://doi.org/10.1021/acssuschemeng.9b01557>.
- [8] Kuo YL, Hsu WM, Chiu PC, Tseng YH, Ku Y. Assessment of redox behavior of nickel ferrite as oxygen carriers for chemical looping process. *Ceram Int* 2013;39:5459–65. <https://doi.org/10.1016/j.ceramint.2012.12.055>.
- [9] Zhao K, Fang X, Huang Z, Wei G, Zheng A, Zhao Z. Hydrogen-rich syngas production from chemical looping gasification of lignite by using NiFe₂O₄ and CuFe₂O₄ as oxygen carriers. *Fuel* 2021;303. <https://doi.org/10.1016/j.fuel.2021.121269>.
- [10] Liu M, Zhang J, Yang T, Rao Q, Gai Z, Zhao J, et al. Light-enhanced thermochemical production of solar fuels from methane via nickel-based redox cycle. *Fuel* 2023;335. <https://doi.org/10.1016/j.fuel.2022.127035>.
- [11] Marcantonio V, De Falco M, Capocelli M, Bocci E, Colantoni A, Villarini M. Process analysis of hydrogen production from biomass gasification in fluidized bed reactor with different separation systems. *Int J Hydrogen Energy* 2019;44:10350–60. <https://doi.org/10.1016/j.ijhydene.2019.02.121>.
- [12] Pallozzi V, Di Carlo A, Bocci E, Villarini M, Foscolo PU, Carlini M. Performance evaluation at different process parameters of an innovative prototype of biomass gasification system aimed to hydrogen production. *Energy Convers Manag* 2016;130:34–43. <https://doi.org/10.1016/j.enconman.2016.10.039>.
- [13] Ma Z, Zhang S, Lu Y. Phase segregation mechanism of NiFe₂O₄ oxygen carrier in chemical looping process. *Int J Energy Res* 2021;45:3305–14. <https://doi.org/10.1002/er.6026>.
- [14] Huang Z, Deng Z, Chen D, Wei G, He F, Zhao K, et al. Exploration of Reaction Mechanisms on Hydrogen Production through Chemical Looping Steam Reforming Using NiFe₂O₄ Oxygen Carrier. *ACS Sustain Chem Eng* 2019;7:11621–32. <https://doi.org/10.1021/acssuschemeng.9b01557>.